Virology 456-457 (2014) 247–258

Contents lists available at ScienceDirect

Virology

journal homepage: www.elsevier.com/locate/yviro

Silencing of neurotropic flavivirus replication in the central nervous system by combining multiple microRNA target insertions in two distinct viral genome regions

Natalya L. Teterina, Guangping Liu, Olga A. Maximova, Alexander G. Pletnev*

Laboratory of Infectious Diseases, National Institute of Allergy and Infectious Diseases, National Institutes of Health, Bethesda, MD 20892, United States

ARTICLE INFO

Article history:
Received 5 February 2014
Returned to author for revisions
28 February 2014
Accepted 1 April 2014
Available online 19 April 2014

Keywords:
Flavivirus
Micrornas
Neuropathogenesis

ABSTRACT

In recent years, microRNA-targeting has become an effective strategy for selective control of tissue-tropism and pathogenesis of both DNA and RNA viruses. Here, using a neurotropic flavivirus as a model, we demonstrate that simultaneous miRNA targeting of the viral genome in the open reading frame and 3′-noncoding regions for brain-expressed miRNAs had an additive effect and produced a more potent attenuation of the virus compared to separate targeting of those regions. Multiple miRNA co-targeting of these two distantly located regions completely abolished the virus neurotropism as no viral replication was detected in the developing brain of neonatal mice. Furthermore, no viral antigens were detected in neurons, and neuronal integrity in the brain of mice was well preserved. This miRNA co-targeting approach can be adapted for other viruses in order to minimize their replication in a cell- or tissue-type specific manner, but most importantly, to prevent virus escape from miRNA-mediated silencing.

Published by Elsevier Inc.

Introduction

The mosquito- and tick-borne viruses of the *Flaviviridae* family represent important emerging and reemerging pathogens such as Japanese encephalitis, St. Louis encephalitis, West Nile, and tick-borne encephalitis (TBEV) viruses that have caused severe neuroinfections with up to 40% mortality in humans in many regions of the world (Lindenbach et al., 2007; Sips et al., 2012). The pathogenesis of neurotropic flavivirus infections involves two distinct properties of the viruses: (i) neuroinvasiveness, which relates to the capacity of the virus to replicate in the peripheral organs, induce viremia, and gain entry to the central nervous system (CNS) and (ii) neurovirulence, which is the ability of the virus to infect and replicate in cells of the CNS and cause encephalitis (Mandl, 2005). In the CNS, the primary targets of neurotropic flaviviruses are neurons (Griffin, 2003). Successful attenuation of a neurotropic virus depends on the prevention of virus entry into the CNS and restriction of its replication in the neurons. In recent years, microRNAs (miRNAs) have emerged as important cellular RNA elements that regulate gene expression at the posttranscriptional level by targeting mRNAs for translational repression or enzymatic degradation. As many cellular miRNAs have a distinctive cell type-specific pattern of expression (Bartel, 2009; Filipowicz et al., 2008; Lagos-Quintana et al., 2002). miRNA targeting of viral genomes has been exploited to restrict virus replication and pathogenesis in a cell- or tissue-specific manner (Kelly and Russell, 2009; tenOever, 2013). Initially tested for picornaviruses (Barnes et al., 2008; Kelly et al., 2008), cell-specific miRNA-dependent suppression of virus replication has proved to be effective *in vivo* for both DNA and RNA viruses (Cawood et al., 2009, 2011; Edge et al., 2008; Kelly et al., 2010a,b; Langlois et al., 2013; Leber et al., 2011; Perez et al., 2009; tenOever, 2013; Ylosmaki et al., 2008, 2013).

Despite the success in controlling viral tissue-tropism and pathogenesis by cellular miRNAs, a major concern for this approach is associated with virus escape from miRNA-mediated inhibition and potential reversion to a virulent phenotype (Barnes et al., 2008; Kelly et al., 2008; tenOever, 2013). We have previously demonstrated that certain miRNAs expressed in the brain can control the neurotropism of a flavivirus bearing perfectly complementary miRNA target sites (Heiss et al., 2011, 2012). Insertion of a single copy of a target for a mir-9, mir-124a, mir-128a, mir-218, or let-7c miRNA into the 3′ noncoding region (3′NCR) of neurotropic chimeric TBEV/Dengue type 4 virus (TBEV/DEN4) was sufficient to block virus replication in the CNS of adult mice and prevent the development of otherwise lethal encephalitis (Heiss et al., 2011). However, the effect of these miRNA target insertions on viral

* Correspondence to: NIAID, NIH, Building 33, Room 3W10A, 33 North Dr., MSC 3203, Bethesda, MD 20892, United States. Tel.: +1 301 402 7754.
E-mail address: apletnev@niaid.nih.gov (A.G. Pletnev).

http://dx.doi.org/10.1016/j.virol.2014.04.001
0042-6822/Published by Elsevier Inc.

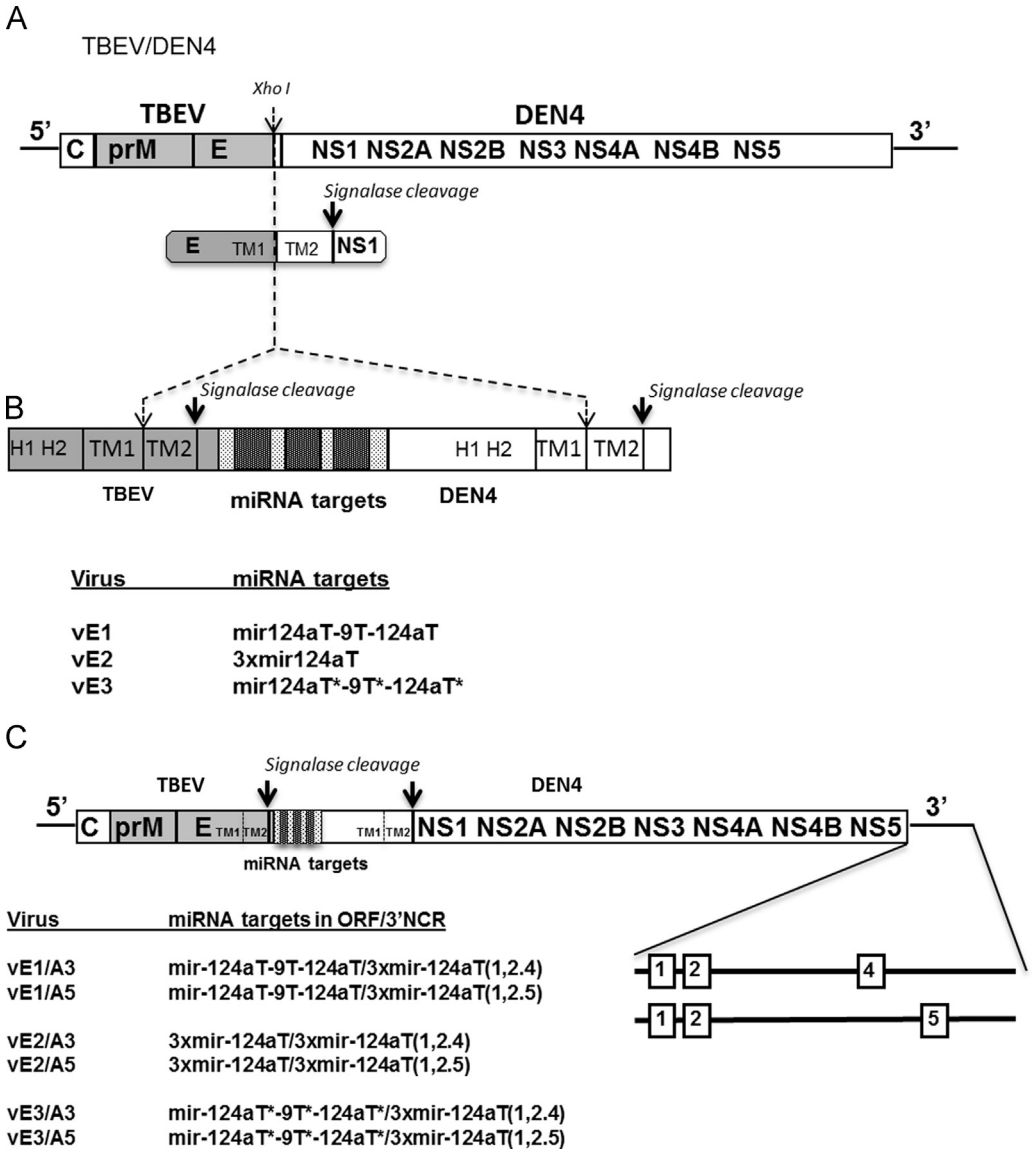

Fig. 1. Schematic representation of viral genomes used in this study. (A) Parental TBEV/DEN4 chimeric virus (Pletnev et al., 1992). Gray area represents TBEV sequences; white area depicts DEN4 virus sequences. Insert shows the junction between the TBEV and DEN4 sequences in the C-terminal end of protein E coding sequence with transmembrane helices TM1 and TM2. Black arrow indicates signalase cleavage site between proteins E and NS1. (B) Schematic illustration of the insertion of target sequences for miRNAs in the area coding for the C-terminal end of protein E. Dashed lines mark sequences inserted at the Xho I site of the parental genome; black arrows indicate duplicated signalase cleavage site; dotted area between TBEV and DEN4 sequences represents inserted miRNA target sequences. (C) Schematic diagram of viruses with combined target sequences in the ORF and 3′NCR. Positions of 3 mir124a target sequences in the 3′NCR are schematically depicted by white boxes.

neurovirulence in newborn mice was less evident, as emerging mutations or deletions within the miRNA target sequences of escape mutants restored the ability of the virus to replicate in the CNS and to cause fatal disease (Heiss et al., 2012). Incorporation of multiple copies of miRNA targets in the 3′NCR and extension of the distance between these targets led to a more effective miRNA-mediated suppression of virus replication. Importantly, the attenuated phenotype was seen even in the developing CNS of suckling mice and in immuno deficient SCID mice that lack potent B and T cell responses (Heiss et al., 2012). However, occasional large deletions of miRNA targets as well as viral genome sequences located between them restored the neurovirulent phenotype in these animal models. These findings prompted us to test whether simultaneous placement of multiple miRNA target sequences at different functionally important regions of the viral genome would greatly reduce or completely prevent virus escape from miRNA-mediated selective suppression. In the present study, we first explored the effect of miRNA targeting in the open reading frame (ORF) of the viral genome, within the region encoding the C-terminal part of the E protein. We next investigated the effects of simultaneous miRNA co-targeting in two distant regions of the viral genome, *i.e.*, in the ORF and 3′NCR. We show here that such combined targeting of the viral genome had an additive effect on reducing neurovirulence of a virus and resulted in no death or neurological signs in newborn mice. No viral replication, neuro degeneration, or virus escape was detected in mouse brains.

Results

Construction of TBEV/DEN4 viruses bearing miRNA targets in the ORF of viral genome

In this study, we explored the ability of cellular miRNAs abundantly expressed in the brain to selectively restrict replication of neurotropic flaviviruses in the CNS by insertion of miRNA

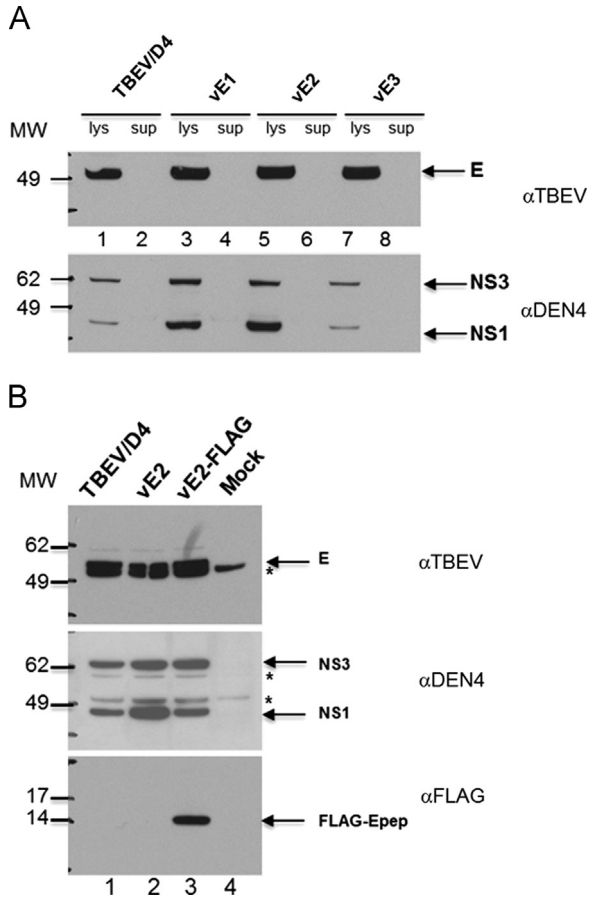

Fig. 2. Immunoblot analysis of viral proteins expressed in Vero cells. (A) Vero cells were infected with TBEV/DEN4, vE1, vE2 or vE3 viruses as specified at the top. After 72 h p.i., cell culture supernatants were collected (sup) and cells were harvested and processed to prepare cell lysates (lys). The samples were analyzed by immunoblotting using antibodies indicated on the right. The positions of molecular weight (MW, in kDa) markers are indicated on the left. (B) Vero cells were infected with TBEV/DEN4, vE2 and vE2-FLAG or mock-infected. After 72 h cells were harvested and cell lysates were processed as described for panel A. The samples were analyzed by immunoblotting using the antibodies indicated on the left. Positions of E, NS3, NS1 proteins and FLAG-tagged C-terminal E protein peptide encoded by insertion (FLAG-Epep) are indicated by arrows on the right side of each panel. * indicates positions of unspecific protein bands recognized by TBEV or DEN4 HAMF in mock-infected cells.

targets in a region of the viral genome inside of the ORF, in the sequence located between TBEV E and DEN4 NS1 protein genes of the chimeric TBEV/DEN4 virus (Pletnev et al., 1992). This chimeric virus contains sequences encoding the structural prM and E proteins of the Far Eastern TBEV with remaining genes derived from mosquito-borne DEN4 virus (Fig. 1). The junction between TBEV and DEN4 sequences at the C-terminal anchor region of protein E was placed so that the first transmembrane helix (TM1) of protein E had the TBEV sequence, while the second transmembrane helix (TM2) contained the DEN4 sequence (Fig. 1A). We designed the insertion of miRNA target sequences in this region using an approach that has been described previously by Bonaldo et al. (2007) for generation of recombinant yellow fever viruses expressing foreign genes (Trindade et al., 2012). The C-terminal stem-anchor (SA) region of protein E (~100 amino acid residues) contains four alpha-helices, two of which (H1 and H2) form a stem region, and two amphipathic anti-parallel α-helices (TM1 and TM2) serve as an E protein membrane anchor and as an internal signal sequence for the cellular signal peptidase cleavage during polyprotein processing (Fritz et al., 2011; Pangerl et al., 2011; Stiasny et al., 2013). Three tandem target sequences for miRNAs were placed between sequences encoding the two SA domains: the first SA domain, located upstream of the miRNA-targets, was a part of the TBEV E protein; the second SA domain, located downstream of the miRNA targets, contained the sequence from the DEN4 E protein (Fig. 1B). Complementary targets for mir-9 and mir-124a miRNAs were selected for insertion into the TBEV/DEN4 genome, since these miRNAs are highly expressed in mouse brains, and insertion of these targets into the chimeric TBEV/DEN4 genome effectively restricted virus replication in neurons and prevented the development of otherwise lethal encephalitis in mice inoculated into the brain (Heiss et al., 2011, 2012). Two variants of miRNA-targeted TBEV/DEN4 viruses were engineered by insertion of the designed synthetic sequences (Fig. S1) into the unique Xho I site of the TBEV/DEN4 cDNA genome (Fig. 1B). The vE1 cDNA carried two targets for mir-124a and one target for mir-9 between them, whereas vE2 cDNA carried three tandem copies of targets for mir-124a. As a control, we generated a third variant vE3 virus, in which miRNA targets of vE1 were modified in each third nucleotide position presumably preventing recognition of these sequences by cellular miRNAs (Fig. S1).

To target viral genomes in two distantly located regions, we also engineered TBEV/DEN4 cDNA genomes in which the above insertions in vE1, vE2, or vE3 were combined with three additional mir-124a targets located in the 3′NCR of the viral genome. We selected and utilized two previously described variants of miRNA-targeting in the 3′NCR of TBEV/DEN4: 3xmir124aT(1,2,4) [designated here as vA3] and 3xmir124aT(1,2,5) [designated here as vA5] that carry three mir-124a binding sites in the 3′NCR at positions 1, 2, and 4 or 1, 2 and 5 (Heiss et al., 2012). Six viruses (designated vE1/A3, vE1/A5, vE2/A3, vE2/A5, vE3/A3, and vE3/A5) were generated from the engineered cDNA genomes as shown in Fig. 1C.

Simian Vero or mosquito C6/36 cells, neither of which expresses the mir-9 or mir-124a miRNAs as measured by TaqMan microRNA assay (Heiss et al., 2011), were able to support the recovery of modified TBEV/DEN4 viruses after transfection with RNAs transcribed from the cDNAs. Viruses were amplified by one additional passage and biologically cloned by two subsequent terminal dilutions. Cloned viruses were amplified in Vero cells by two or three additional passages and reached a titer of at least 10^8 PFU/ml. Genetic stability of the insertions in the genomes of the produced recombinant viruses was evaluated by additional multiple passages in Vero cells at low multiplicity of infection (0.01 PFU/cell). All viruses were genetically stable and contained the designed insertions as verified by sequence analysis of viral RNA genomes determined after 6, 8, and 10 passages in Vero cells.

Expression of viral proteins in Vero cells

To determine if viral polyproteins were proteolytically processed correctly in cells infected with vE1, vE2 and vE3 viruses bearing insertions in the ORF, we examined viral protein expression in infected cells by Western blot analysis. Vero cells were infected with each modified or parental virus at an MOI of 0.5, and cell lysates and supernatants were analyzed on day 3 p.i. The immunoblot patterns revealed that TBEV E protein and DEN4 NS1 and NS3 proteins of the TBEV/DEN4 parental virus and vE1, vE2, and vE3 derivative viruses co-migrated by SDS–PAGE (Fig. 2A), indicating correct processing of polyprotein. The expected polypeptide band corresponding to the product encoded by insertion in vE1, vE2, or vE3 and containing the DEN4 SA region of the E protein was not detected by TBEV- or DEN4-specific antibodies. To verify the expression of this new polypeptide, we added the sequence encoding the commonly used FLAG-tag epitope upstream of the miRNA target sequences in each of the three recombinant viruses, generating vE1-FLAG, vE2-FLAG, and

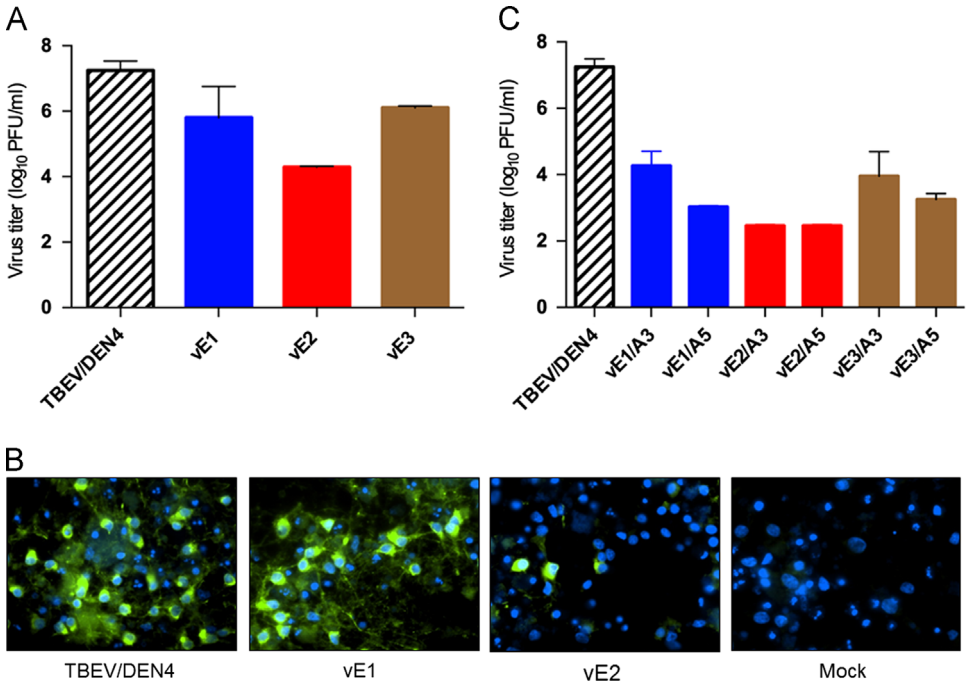

Fig. 3. Effect of miRNA target insertions on TBEV/DEN4 virus replication in primary neuronal cells. (A and C) Neuronal cells were infected at MOI of 0.5 with the indicated viruses, and culture medium was collected at 72 h p.i. Virus titers in culture medium were determined by PFA on Vero cells. Values for each virus, determined in triplicates in the same experiment, are shown with corresponding standard deviations. (B) TBEV antigen (TBEV-Ag) expression in primary neuronal cells detected by immunofluorescence assay with αTBEV HMAF four days after infection with the indicated viruses or mock inoculated. TBEV-Ag – green, DAPI – blue.

vE3-FLAG viruses. As shown in Fig. 2B, the expected polypeptide of ~14 kDa was detected and specifically recognized by the mouse monoclonal anti-FLAG antibodies in the lysates of cells infected with vE2-FLAG. Similar bands were observed for cells infected withvE1-FLAG and vE3-FLAG (data not shown). The anti-FLAG antibodies did not detect any additional bands of higher molecular weight corresponding to potential intermediate products containing a cleavage site for the cellular signalase. These results suggest a complete and correct processing of the viral E and NS1 proteins from the polyprotein precursor.

Replication of miRNA-targeted viruses in primary neuronal cells

To evaluate miRNA-mediated restriction of virus replication *in vitro*, growth of parental TBEV/DEN4 and engineered viruses was monitored in primary neuronal cells derived from the embryonic rat cortex which express high levels of mir-9 and mir-124a miRNAs (Krichevsky et al., 2003). Parental TBEV/DEN4 virus and the vE3 derivative with the scrambled miRNA target sequences replicated efficiently in these cells, reaching virus titers of 7.0 and 6.1 $\log_{10}$ PFU/ml, respectively, by day 3 p.i. Insertion of three copies of the mir-124a targets in the ORF of the vE2 virus significantly impaired virus replication in neuronal cells, as the yield of vE2 virus was reduced by ~1000- or 100-fold compared to that of parental virus or control vE3 virus, respectively (Fig. 3A). Immunostaining of TBEV antigens in the infected cells demonstrated that replication of the vE2 virus was significantly restricted in the majority of cells (Fig. 3B). Surprisingly, targeting of the viral genome in the same site for two different miRNAs (mir-9 and mir-124a) did not produce such restriction of virus replication. The levels of replication for both vE1 mutant and control vE3 virus were similar indicating that such combination of miRNA targets (mir-124aT-9T-124aT) placed within the ORF of the viral genome was not effective for viral attenuation *in vitro*. Sequence analysis of the viral RNAs isolated from the supernatants of neuronal cells at 72 h post-infection demonstrated the presence of input viruses (vE1 or vE2) together with their corresponding escape deletion mutants that lost all inserted miRNA target sequences. However, the genome of the control virus E3 remained stable during replication in neuronal cells (data not shown).

When three miRNA target sequences in the ORF were combined with three additional mir-124a targets in the 3′NCR, an additive effect on the restriction of virus replication in neuronal cells was manifested. Replication of the viruses vE2/A3 and vE2/A5, with 6 copies of mir124aT, was decreased a further50- and100-fold compared to that of viruses carrying 3 copies of target sequences either in the ORF (vE2 virus; Fig. 3A) or the 3′NCR (vE3/A3 and vE3/A5; Fig. 3C) alone.

Neurovirulence of viruses with miRNA targets inserted in the ORF

The neurovirulence of the recombinant viruses was evaluated in suckling mice, a most sensitive animal model for assessment of flavivirus neurovirulence. As shown in Table 1, targeting the viral genome inside of the ORF with three copies of target sequence for the brain-expressed mir-124a resulted in substantial attenuation of vE2 in newborn mice. Of 30 mice that received an intra cerebral dose of 10, 100, or 1000 PFU, only three mice developed neurological signs (limb weakness or paralysis), while the rest of the mice remained asymptomatic during the 21 day observation period. The IC LD_{50} of vE2 virus was greater than 1000 PFU and increased over 1250-fold compared to parental TBEV/DEN4 virus [IC LD_{50} of 0.8 PFU (Heiss et al., 2012)]. The neurovirulence of the control vE3 virus carrying scrambled miRNA targets remained high (LD_{50} of 23.7 PFU), indicating that the attenuation phenotype of vE2 is specific and determined by the presence of three mir-124a target sequences. At the same time, substitution of one mir-124a target sequence in the vE2 with the target sequence for another brain-expressed miRNA (mir-9) significantly decreased the attenuation effect, as observed for vE1 (an estimated IC $LD_{50}$for vE1 was 44.7 PFU).

Table 1
Neurovirulence of chimeric TBEV/DEN4 miRNA-targeted viruses in suckling mice.

Virus	Group[a]	Dose (PFU)	No. of moribund mice on the indicated day (dpi)[b]	Morbidity (%)	LD_{50} (PFU)	Fold reduction[c]
vE1	1–1	10	2(d14)	20	44.7	56
	1–2	10^2	3(d10), 3(d11), 2(d13)	70		
	1–3	10^3	5(d10), 4(d11)	90		
vE2	2–1	10		0	> 1000	> 1250
	2–2	10^2	1(d14)	10		
	2–3	10^3	1(d15), 1(d18)	20		
vE3	3–1	1		0	23.7	30
	3–2	10	1(d10), 1(d15)	20		
	3–3	10^2	10(d10)	100		
vE1/A3	4–1	10		0	> 1000	> 1250
	4–2	10^2		0		
	4–3	10^3		0		
vE1/A5	5–1	10		0	> 1000	> 1250
	5–2	10^2		0		
	5–3	10^3		0		
vE2/A3	6–1	10		0	> 1000	> 1250
	6–2	10^2		0		
	6–3	10^3		0		
vE2/A5	7–1	10		0	> 1000	> 1250
	7–2	10^2		0		
	7–3	10^3		0		
vE3/A3	8–1	10		0	> 100	> 125
	8–2	10^2	1(d15)	10		
vE3/A5	9–1	10		0	> 1000	> 1250
	9–2	10^2	1(d14), 1(d17)	20		
	9–3	10^3		0		
TBEV/DEN4	10	10	6(d8), 4(d9)	100	0.8[d]	

[a] Groups of 10 3-day-old Swiss mice were inoculated IC with the indicated dose of virus.
[b] The brains of paralyzed mice were collected on the indicated day, and viral RNA was isolated from brain homogenate and directly used for sequence analysis. The results of sequence analysis of brain-derived escape mutant viruses are shown in Fig. S2 in the supplemental material.
[c] Fold reduction in neurovirulence for each miRNA-targeted virus compared to that of the TBEV/DEN4 parent.
[d] The IC LD_{50} of TBEV/DEN4 from the previous studies (Engel et al., 2010; Heiss et al., 2012).

Combined miRNA-targeting in the ORF and 3′NCR had an additive effect and resulted in a more profound reduction of neurovirulence of TBEV/DEN4 virus in newborn mice. No death or neurological signs were observed in mice inoculated into the brain with 10, 100, or 1000 PFU of vE1/A3, vE1/A5, vE2/A3, or vE2/A5. Also, two viruses (vE3/A3 and vE3/A5) with 3 copies of mir-124a target sequences in the 3′NCR and scrambled miRNA targets in the ORF exhibited substantial attenuation in newborn mice, similar to that observed for viruses (vA3 and vA5) with the same combination of target sequences in the 3′NCR alone (Heiss et al., 2012). Only 1 or 2 of 30 mice infected with vE3/A3 or vE3/A5 viruses, respectively, developed paralysis after a longer incubation period compared to that of mice infected with the TBEV/DEN4 parent (Table 1).

On day 22, the brains of five surviving mice were collected from each group (groups 4-3, 5-3, 6-3, 7-3, 8-2, and 9-3; Table 1) that was infected with the highest dose. Each individual brain suspension was tested in Vero cells for the presence of infectious virus. Infectious virus was isolated only from the brain of one of five animals injected with vE3/A5 virus. Sequence analysis of this isolate identified alarge deletion (339 nts) in the 3′NCR that began close to the TAA stop codon of the ORF and included the introduced three mir-124a targets and genome sequence located between them. The brains from all other animals were free from inoculated virus as determined by plaque assay or RT-PCR analysis, and no virus was isolated after additional blind passage on Vero cells.

These results indicate that simultaneous multiple miRNA targeting of the viral genome within the ORF and 3′NCR produces a strong attenuating effect on virus neurovirulence and is sufficient to prevent virus escape from miRNA-mediated suppression in the brain.

Genetic stability of miRNA-targeted viruses in the CNS

Virus escape from miRNA pressure in the CNS by accumulation of mutations or deletions within the miRNA targets is a common occurrence among viruses carrying target sequences in the 3′NCR (Barnes et al., 2008; Heiss et al., 2011, 2012; Lauring et al., 2010; Ylosmaki et al., 2013). Here, we examined whether the onset of viral encephalitis observed in suckling mice inoculated with viruses bearing miRNA targets in the ORF was the result of a similar process. We sequenced the region encoding the C-prM-E-NS1 proteins of 19 viruses isolated from brains of individual mice that succumbed to the IC infection (Table 1). The sequence analysis results are shown in Fig. S2 in the supplemental material. Sequences of viral RNAs derived from the brains of four moribund mice infected with the control vE3 virus, were identical to the sequence of the input virus, indicating that the inserted sequences of the scrambled miRNA targets were stable during virus

replication in the mouse brain. Also, in six of the 13 brain-derived vE1 isolates, no mutations or deletions were detected. However, seven vE1 isolates as well as two vE2 brain-derived viruses contained large deletions (from 81 to 603 nts). The observed deletions can be divided in two groups. In the first group, relatively short deletions were found in vE2-Δ81, vE1-Δ147, vE1-Δ165, vE1-Δ219, and vE1-Δ270 escape mutants that partially eliminated sequences located between the two encoded sites for signalase cleavage and including the miRNA targets (Figs. 4 and S2). With the exception of the vE1-Δ219 virus, all these escape mutants were infectious for Vero cells and replicated to titers of at least 10^6 PFU/ml when amplified in cells at 37 °C. The second group of brain-derived viruses (vE2-Δ447, vE1-Δ402, and vE1-Δ411; Fig. 4) acquired larger deletions, which included stem-anchor structural elements of the TBEV E protein and the E/NS1 signalase cleavage site (Fig. S2). These viruses contained chimeric E proteins with the H1 sequence of TBEV, TM1 and TM2 sequences from DEN4, and a newly formed H2 stem helix. Joining of TBEV and DEN4 H2 remnants resulted in the variable size of this element (*e.g.*, an increase in theH2 size by 7 amino acids in vE1-Δ411 or a decrease by 4 amino acids in vE2-Δ447).

Multiple site miRNA co-targeting within the ORF and 3′NCR greatly restricts virus replication and prevents neuronal degeneration in the CNS

Previous studies had demonstrated that increasing the number of mir-124a targets to four copies in the 3′NCR significantly diminished virus replication (Heiss et al., 2012). In the current study, we explored whether the insertion of 6 miRNA binding sites in two regions (ORF and 3′NCR) of the viral genome would further reduce virus replication in the brain and minimize virus-induced neuronal damage.

Three-day old mice were inoculated IC with 10^3 PFU of each of the following viruses: vE1/A3, vE1/A5, vE2/A3, vE2/A5, vE3/A3, or vE3/A5. The brains of three mice from each group were collected on days 8, 13, and 20, and virus loads in each individual brain were determined by titration on Vero cells. We have previously shown that the TBEV/DEN4 virus rapidly achieved high titers (10.2 $\log_{10}$ PFU/g of brain) and caused paralysis or death by day 7 p.i. when inoculated IC at this high dose (Engel et al., 2010; Heiss et al., 2012). Replication of the viruses with multiple complementary miRNA targets within the ORF and 3′NCR (*i.e.*, vE1/A3, vE1/A5, vE2/A3, and vE2/A5 viruses) was below the level of detection (< 1.7 $\log_{10}$ PFU/g) and all mice remained healthy (Fig. 5). At the same time, viruses with scrambled miRNA target sequences in the ORF (*i.e.*, vE3/A3 and vE3/A5) were able to replicate, albeit to low levels (up to 2.7 $\log_{10}$ PFU/g) and without producing any clinical signs (Fig. 5).

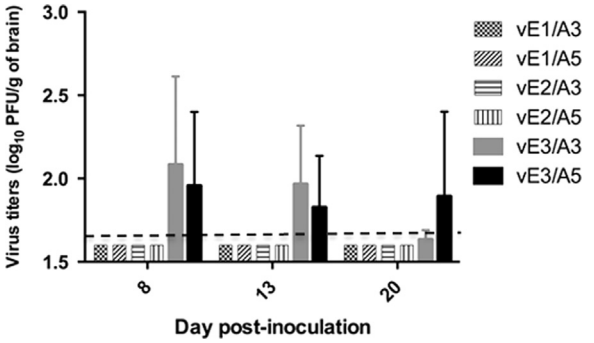

Fig. 5. Replication kinetics of recombinant TBEV/DEN4 viruses with miRNA target sequences within the ORF and 3′NCR in mouse brain. 3-day-old Swiss mice were inoculated IC with 1000 PFU of the indicated viruses. Brains were collected from three mice in each group on day 8, 13 and 20, and virus titers were determined by PFA on Vero cells. The limit of detection (1.7 $\log_{10}$ PFU/g of brain) is indicated by the dashed line.

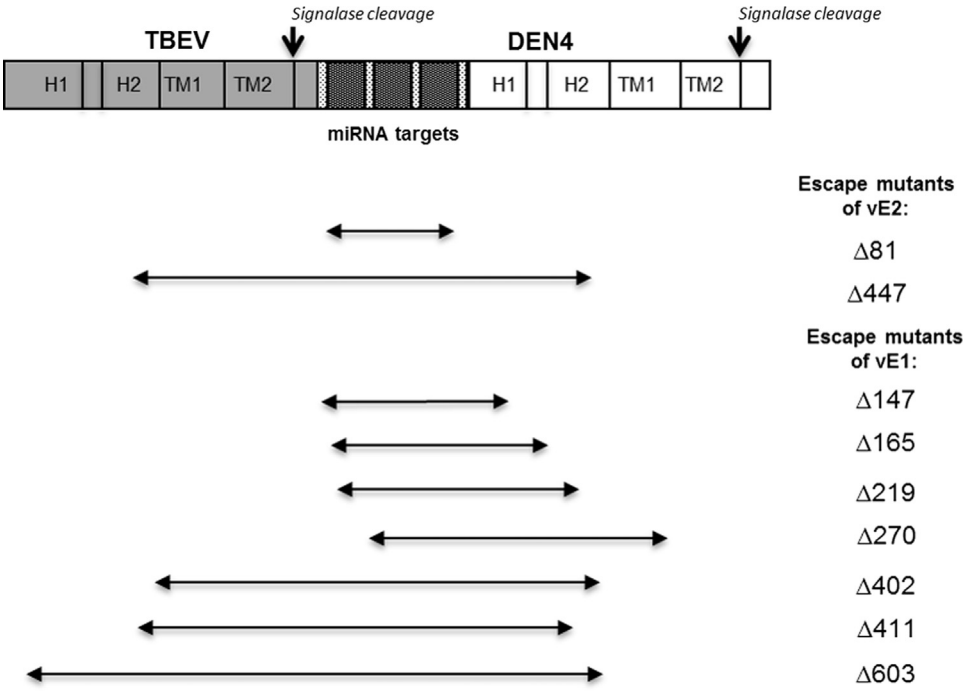

Fig. 4. Location and size of the deletions in the ORF of escape mutants detected in the brains of moribund mice infected IC with miRNA-targeted viruses. Schematic diagram of the insertion of target sequences for miRNAs in the area encoding the C-terminal end of protein E. Dotted lines mark sequences inserted at the Xho I site of the parental genome; black arrows indicate duplicated signalase cleavage sites; dotted area between TBEV sequences (shown in gray) and DEN4 sequences (illustrated in white) represents inserted miRNA target sequences. The size of the deletions detected in the isolated escape mutants (number of nucleotides deleted) is shown in the right column and their locations in the ORF are indicated by double head arrows. Amino acid sequences for each deletion mutant are shown in Fig. S2 in the supplemental material.

We next analyzed the distribution of viral antigens and virus-induced histopathology in the brains of infected mice. Simultaneous immunostaining of multiple mouse brains (MultiBrain Technology, NeuroScience Associates) for the TBEV viral antigens corroborated the data on virus replication (Fig. 6). Various neuronal populations throughout the brain of mice infected with the parental TBEV/DEN4 virus displayed massive amounts of viral antigens (Fig. 6C–I). In line with the low levels of detected infectious virus, viral antigens of the vE3/A3 and vE3/A5 virus were detected only in very small amounts in some cortical neurons and Purkinje cells (Fig. 6J and L; vE3/A5 virus is shown). No viral antigens were detected in neurons of mice inoculated with the vE1/A3, vE1/A5, vE2/A3, or vE2/A5 virus at any time point (Fig. 6A and B; vE2/A3 is shown).

The extent of histopathological changes also correlated well with the virus titers and amounts of viral antigens observed. The parental TBEV/DEN4 virus induced extensive damage to neuronal somatodendritic compartments and microgliosis (Fig. 7B). In mice inoculated with the vE1/A3, vE1/A5, vE2/A3, or vE2/A5 virus, the integrity of neuronal somatodendritic compartments was well preserved and microglia maintained its "quiescent/surveying" phenotype (compare Fig. 7C, E2/A3 virus, and Fig. 7A, Mock). The brains of mice inoculated with the vE3/A3 or vE3/A5 virus also did not show signs of neuronal damage, but microglia appeared activated, albeit to a much lesser extent than in the TBEV/DEN4-infected mice (Fig. 7C, vE3/A5 virus is shown). Since microglia are very sensitive to even minor insults, the microglial morphology seen in mice infected with the vE3/A3 or vE3/A5 virus is indicative of ongoing low-level virus replication of these viruses.

Taken together, these findings clearly demonstrate that multiple miRNA co-targeting in the ORF and 3′NCR leads to inability of the targeted virus to establish a productive neuroinfection.

Multiple miRNA target insertions within the ORF and 3′NCR do not disrupt virus immunogenicity and protective efficacy

To determine the ability of the TBEV/DEN4 viruses with a combination of six miRNA targets in ORF and 3′NCR to replicate in the periphery and induce protective immunity, adult immunocompetent Swiss female mice in groups of 10 were inoculated IP with a 10^5 PFU dose of parental TBEV/DEN4 or miRNA-targeted virus. All mice remained healthy during the 28-day observation period and developed a moderate level of TBEV-specific neutralizing antibodies in serum (from 1:10 to 1:26 as determined by plaque reduction neutralization assay 60%). On day 29, mice were challenged with 100 IP LD_{50} of the neuroinvasive TBEV/LGT virus (IP LD_{50} of 32 PFU was determined in 3-week-old mice) and observed for an additional 28 days for morbidity and mortality. All mice immunized with vE1/A3, vE1/A5, vE2/A3, vE2/A5, or

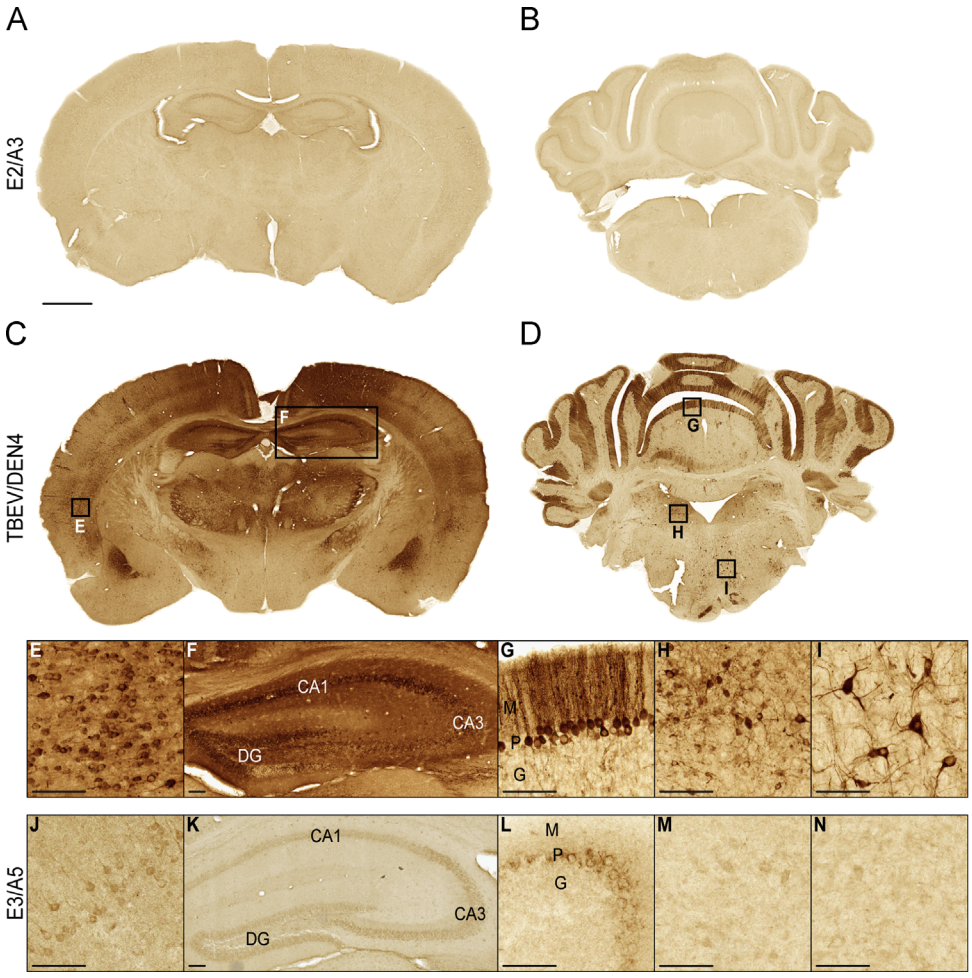

Fig. 6. Distribution of viral antigens in neurons of infected mice. Immunohistochemical detection of the TBEV antigens is shown in representative brain sections from a mouse IC inoculated with the vE2/A3 virus (A and B; 20 dpi), parental TBEV/DEN4 virus (C–I; 6 dpi), or the vE3/A5 virus (J–N; 20 dpi). Boxed areas in (C) and (D) are shown at higher magnification in (E) (cerebral cortex), (F) (hippocampus), (G) (cerebellar cortex), (H) (medial vestibular nucleus), and (I) (reticular nucleus). (J–N) The same brain areas are shown at high magnification for a mouse inoculated with E3/A5 virus. Abbreviations: DG, dentate gyrus; CA1 and CA3, areas of hippocampus; M, molecular layer; P, Purkinje cell layer; G, granule cell layer. Bar in (A) (1 mm) also applies to (B)–(D). Bars in (E)–(N): 100 μm.

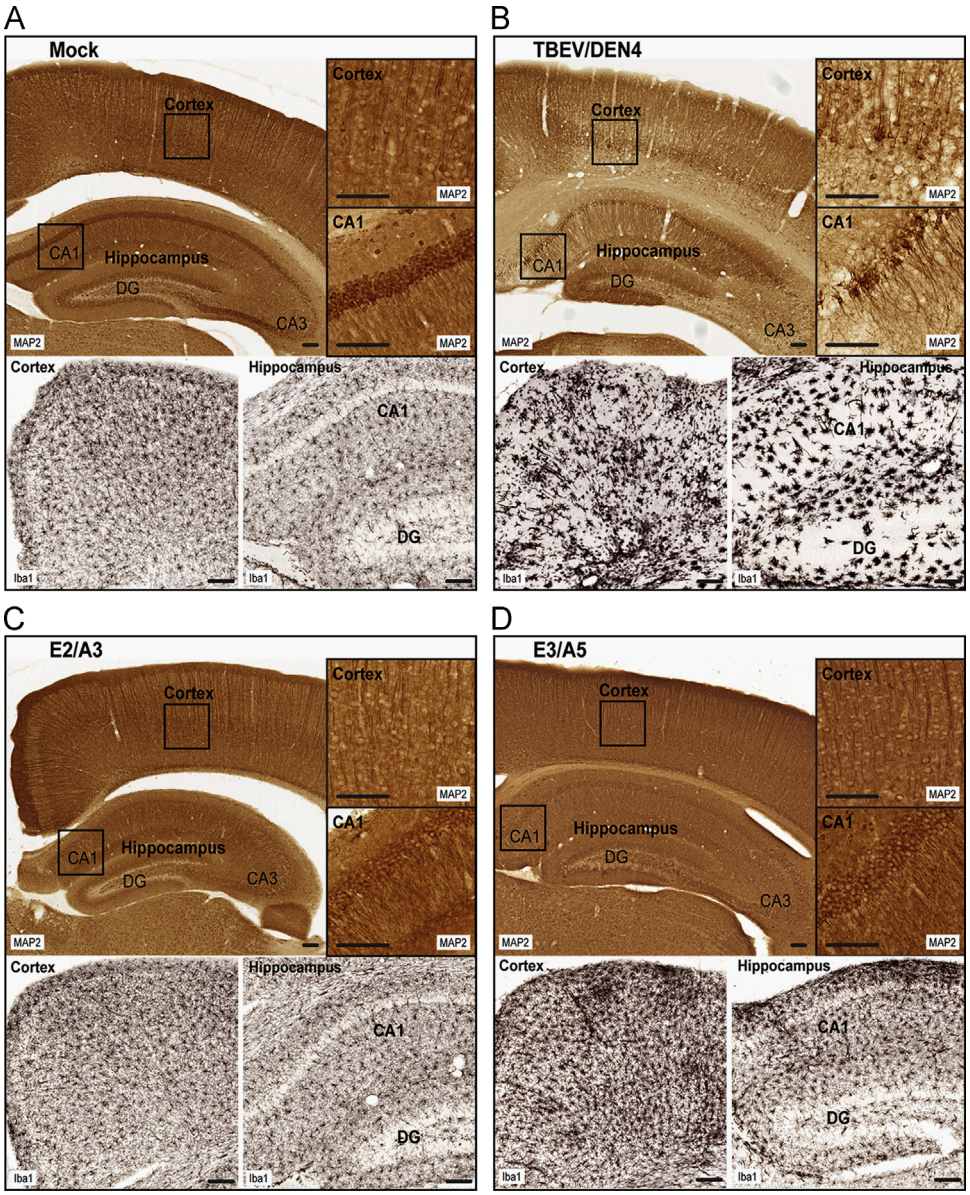

Fig. 7. Extent of neuronal damage and microgliosis in the mouse brain. Immunostaining for the microtubule-associated protein 2 (MAP2) reveals the somatodendritic neuronal compartments. Immunostaining for the ionized calcium binding adapter molecule 1 (Iba1) reveals microglial morphology. Representative sections of the cerebral cortex and hippocampus are shown from a mock-inoculated mouse (A; 20 dpi) or mice infected with the TBEV/DEN4 (B; 6 dpi), vE2/A3 virus (C; 20 dpi), or vE3/A5 (D; 20 dpi) virus. Boxed areas of the MAP2-IR are shown at higher magnification in the corresponding insets on the right. Representative areas of the Iba1-IR are also included in each panel. Dentate gyrus (DG) and CA3 area of hippocampus are also indicated. Bars: 100 μm.

parental TBEV/DEN4 virus survived. To determine whether there was an age-related resistance of mice to the TBEV/LGT challenge, a mock-inoculated group of the same age mice as those immunized served as controls. Eight of ten mice from the control group died and two mice developed clinical signs of morbidity (ruffed fur, hunched back and slow movement) during the 28-day observation after challenge. Thus, mice immunized with a single dose of TBEV/DEN4 parent or any of its multiple miRNA-targeted viruses were completely protected against challenge with neuroinvasive TBEV/LGT virus.

Discussion

MicroRNA targeting provides an effective method to restrict virus replication in a tissue-specific manner, and the concept of miRNA-mediated control of virus tissue-tropism and pathogenesis has been successfully demonstrated for various viruses that replicate in peripheral organs (Edge et al., 2008; Kelly et al., 2008, 2010b; Kelly and Russell, 2009; Langlois et al., 2013; Leber et al., 2011; Perez et al., 2009; Pham et al., 2012; tenOever, 2013; Ylosmaki et al., 2008). Silencing of miRNA-targeted viruses might be a result of both delay of virus replication caused by the miRNA-specific suppression, and rapid virus clearance by host immune responses. In many instances, the selective pressure of cellular miRNAs on the virus replication was strong and effective, and the emergence of escape mutant viruses was not observed (Edge et al., 2008; Kelly et al., 2010b; Langlois et al., 2012, 2013; Perez et al., 2009). However, the possibility of virus escape by accrual of mutations in the miRNA-target sequence and reversion to a virulent phenotype raised a concern about this approach, particularly when it is applied to control neurotropic virus infection in the CNS (Barnes et al., 2008; Heiss et al., 2011, 2012; Yen et al., 2013; Ylosmaki et al., 2013). The normal CNS is structurally isolated from

the immune system and protected by the blood–brain and blood–cerebrospinal barriers that limit, but do not exempt the CNS from immunological surveillance (Mrass and Weninger, 2006; Ousman and Kubes, 2012). A variety of factors, including the immune system maturity and levels of miRNA expression and distribution in the CNS, may play a role in the control of miRNA-targeted virus replication in the host. Our previous findings demonstrated that viral replication and neuronal damage induced by a neurotropic flavivirus, chimeric TBEV/DEN4 virus, can be selectively attenuated for the CNS of mice by inserting target sequences for neuron-specific miRNAs in the 3′NCR of the viral genome (Heiss et al., 2011, 2012). The degree of virus attenuation for the CNS can be proportionally enhanced by increasing the number of miRNA target sites and targeting a large portion of the 3′NCR. This strategy improved the effectiveness of virus suppression by delaying its replication in the developing CNS of newborn mice, thus providing a prolonged time for virus clearance by the immune system. However, miRNA-targeted TBEV/DEN4 viruses occasionally overcame the antiviral activity of miRNAs and escaped from miRNA-mediated suppression by deletion of the inserted miRNA targets and the viral sequences located between them. This finding prompted us to place multiple miRNA target sequences into different functionally important regions of the virus genome to test whether such targeting would prevent virus escape. Suppression by targeting in the 5′NCR and ORF appears to be less frequent than 3′NCR targeting and generally less effective, possibly due to ribosome interference with the RNA-induced silencing complex (RISC) at the translated mRNA sequence (Bartel, 2009; Filipowicz et al., 2008). However, recent studies on miRNA regulation of mRNA translation have demonstrated that miRNA suppression in the coding region can be functional (Fang and Rajewsky, 2011). In the present study, we first evaluated the placement of target sequences for brain-expressed miRNAs in the coding region of the TBEV/DEN4 genome between the genes encoding the E and NS1 proteins and then studied the effect of simultaneous co-targeting of the viral genome within the ORF and 3′NCR. We found that such modifications of the viral genome do not affect normal polyprotein processing and the viruses (vE1, vE2 and control vE3) were stable during multiple passages in Vero cells. In addition, analyses of viruses derived from the brains of moribund mice inoculated with the control virus vE3 containing scrambled miRNA target sequences demonstrated that such insertions in the ORF are stable during virus replication *in vivo*. Targeting in the ORF with three tandem copies for brain-expressed mir-124a (vE2) was most efficacious for attenuation of virus replication in primary neuronal cells and neurovirulence in neonatal mice. However, the substitution of one copy of mir-124a target by the target for another brain-expressed miRNA (mir-9) in vE1 virus considerably decreased the observed attenuation effect both *in vitro* and *in vivo*. This was rather surprising, as in previous studies we have shown that tandem insertion of mir-9 and mir-124a target sequences in the 3′NCR produced a greater attenuating effect than tandem insertion of three synonymous mir-124a target sequences (Heiss et al., 2012). Many factors could contribute to the effectiveness of miRNA-mediated mRNA translational suppression when the target sites are relocated into different regions of the genome or mRNA (Bartel, 2009; Fang and Rajewsky, 2011; Lin and Ganem, 2011; Pasquinelli, 2012). miRNA-target sequence accessibility for RISC binding, distances between miRNA targets, and interactions between RISCs pre-loaded with identical and/or different miRNAs, can interfere with miRNA-recognition and binding to targeted mRNAs (Bartel, 2009; Filipowicz et al., 2008; Kelly and Russell, 2009; Pasquinelli, 2012; Saetrom et al., 2007). We speculate that insertion of the mir-9T sequence between twomir-124aT sequences in vE1 did not give the expected increase in virus suppression *in vivo* and *in vitro* due to adverse local RNA conformational changes, which may cause steric hindrance of RISC-binding to the target sequences. The absence of mutations in the miRNA-target region of six out of 13 (46%) brain-derived viruses from mice that succumbed to the vE1 infection supports this notion, suggesting a limited involvement of miRNA-machinery in the vE1 virus suppression compared to that of the vE2 virus. Nevertheless, in the remaining seven out of 13 moribund mice infected with vE1, severe neurological disease was associated with emergence of escape mutants in the brains. Emerging TBEV/DEN4 mutant viruses escaped the miRNA-mediated suppression by deleting all miRNA-targets located between the TBEV E and DEN4 NS1 protein genes. These findings are in line with our previous observations of virus escape *via* deletion of miRNA-target sequences in the 3′NCR during replication in the CNS (Heiss et al., 2011, 2012).

Analysis of the sequences of escape vE2 and vE1 mutants provides new insight into the structural requirements for the stem-anchor (SA) domain of the envelope protein E, as in several instances we observed the emergence of viruses containing chimeric E protein with various combinations of TBEV and DEN4 SA domain sequences (escape viruses vE2-Δ447, vE1-Δ402 and vE1-Δ411). Both stem (H1 and H2 helices) and transmembrane anchor (TM1 and TM2 helices) regions are believed to be involved and play an active role in the formation of the E protein trimer and the fusion to endosomal membrane during virus entry into the cell (Fritz et al., 2011; Pangerl et al., 2011; Stiasny et al., 2013). Fritz et al. (2011) recently demonstrated that the TM1 and/or TM2 regions of the TBEV E protein can be substituted by the corresponding sequences derived from a distantly related flavivirus (Japanese encephalitis virus), but this resulted in dramatic reduction of virus growth in mammalian cells. Here, we found that a much larger C-terminal part of TBEV E protein in vE1-Δ411 and vE2-Δ447 was replaced by the sequence derived from mosquito-borne DEN4 virus without negative impact on virus growth. These rearrangements in the SA region did not affect virus replication since both viruses were able to grow in Vero cells to high titers ($\sim 10^7$ PFU/ml), similar to that of TBEV/DEN4 virus (data not shown). Another interesting observation derived from the analysis of the escape mutants is related to requirements for size and content of the SA domain inserted between two E/NS1 signalase cleavage sites that can support correct polyprotein processing. Sequence analysis of vE1-Δ270 indicates that this escape mutant has lost the entire DEN4 stem region and contained only 55 amino acid residues between two E/NS1 signalase cleavage sites corresponding to the truncated DEN4 TM1 and intact TM2 region. Such virus also initiated productive infection and replicated in Vero cells suggesting that proper polyprotein processing occurred.

Multiple miRNA co-targeting of the viral genome within the two distantly located regions (the ORF and 3′NCR) completely abolished the neurotropism of virulent TBEV/DEN4 virus in mice. Importantly, insertion of multiple miRNA-targets in vE1/A3, vE1/A5, vE2/A3, and vE2/A5 viruses did not affect their protective efficacy, since mice immunized with a single dose of any of these viruses were completely protected against severe IP challenge with neuroinvasive TBEV/LGT virus. Our studies in neonatal mice demonstrated that extensive miRNA co-targeting of viral genomes in the ORF and 3′NCR had an additive effect and produced a more potent attenuation of neurovirulence compared to separate targeting of those regions. No viral replication was detected in the developing mouse brain after infection with viruses carrying six targets for brain-expressed miRNAs. Furthermore, no viral antigens were detected in neurons of mice intracerebrally inoculated with such viruses, and the integrity of neuronal somatodendritic compartments in the brain appeared well preserved.

In conclusion, we describe here an effective approach to attenuate the pathogenicity of neurotropic viruses which prevents

virus escape and reversion to a neurovirulent phenotype. TBEV/DEN4 viruses with six copies of target sequences for brain-expressed miRNA within the ORF and 3′NCR were unable to replicate in neurons *in vivo*; however, they induced a humoral antibody response in immunized mice and provided protection against subsequent challenge with neurovirulent virus. This approach can be adapted for other viruses in order to minimize their replication in a cell type specific manner, but most importantly, to prevent virus escape from miRNA-mediated silencing.

Materials and methods

Viruses

All miRNA-targeted viruses were derivatives of an infectious cDNA clone of chimeric TBEV/DEN4 virus (GenBank access # FJ28986) (Pletnev et al., 1992) generated using reverse genetics technology. In the chimeric TBEV/DEN4 virus, the sequence encoding the structural prM and E proteins of mosquito-borne Dengue type 4 (DEN4) virus was replaced with the corresponding region (nucleotides (nt) 415–2376) derived from the Far Eastern TBEV strain Sofjin. Recombinant chimeric TBEV/LGT virus was created by replacing the prM and E structural protein genes of the highly attenuated E5 strain of tick-borne Langat virus (LGT) (Pletnev, 2001) with the corresponding TBEV genes derived from the TBEV/DEN4 chimera. (Construction of the TBEV/LGT will be published elsewhere.) The TBEV/DEN4 cDNA contains aunique Xho I site at nucleotide (nt) position 2364, at the junction between the TBEV and DEN4 sequences in the E protein gene (Fig. 1A). Insertion of the synthetic sequence E1 (Fig. S1 in the supplemental material) (Blue Heron Biotechnology) at this site resulted in the TBEV/DEN4-E1 virus (designated vE1) carrying three complementary miRNA targets between the sequence encoding the TBEV envelope E protein and the sequence encoding the DEN4 non-structural protein NS1 (Fig. 1B). Specifically, the introduced E1 sequence encoded 25 C-terminal amino acids of protein E and 10 N-terminal amino acids of protein NS1 of TBEV, followed by three targets for cellular miRNAs expressed in brain tissue (one target (T) for mir-9 and two Ts for mir-124a), and then by the sequence encoding 73 amino acids from the C-terminal end of the DEN4 E protein. Recombinant cDNA genomes of TBEV/DEN4-E2 or TBEV/DEN4-E3 (designated vE2 or vE3, respectively) were generated by replacement of the BsiWI-SfiI fragment of vE1 cDNA with a 110 nt synthetic E2 sequence containing three targets for mir-124a miRNA, or with an E3 sequence containing scrambled target sequences for mir-9 and mir-124a (Fig. S1). The vE1-FLAG cDNA was generated by substitution of the XhoI-BsiWI DNA fragment in the vE1 cDNA with a synthetic 139 nt fragment E-FLAG (Blue Heron Biotechnology) (Fig. S1) containing 76 nts of the 3′ end of a TBEV protein E gene, 30 nts of the 5′ end of NS1 coding sequence and 24 nts encoding FLAG-tag (DYKDDDDK). The same strategy was used to generate the vE2-FLAG and vE3-FLAG cDNAs. Two miRNA-targeted viruses, TBEV/DEN4 3x mir124aT(1,2,4) [designated vA3] and TBEV/DEN4 3x mir124aT(1,2,5) [designated vA5], were constructed previously (Heiss et al., 2012) and used in this study to generate TBEV/DEN4 viruses for simultaneous multiple targeting of the virus genome in the 3′NCR and ORF between the TBEV E and DEN4 NS1 genes. The DNA fragment from vA3 or vA5 cDNA that contained the 3′NCR with inserted 3x mir-124a targets at the sites 1,2,4 or sites 1,2,5 (Heiss et al., 2012) was used for replacement of the corresponding sequence in the full-length cDNA genomes of vE1, vE2, or vE3. Full-length cDNA of four newly engineered viruses (designated vE1/A3, vE1/A5, vE2/A3, and vE2/A5) carrying 6 miRNA targets and two viruses (vE3/A3 and vE3/A5) carrying three miRNA-targets in the 3′NCR and scrambled target sequences between TBEV E and DEN4 NS1 protein genes were constructed, as shown in Fig. 1C.

RNA transcripts generated from modified TBEV/DEN4 cDNAs were used to transfect monolayers of Vero cells in the presence of Lipofectamine as described previously (Engel et al., 2010; Rumyantsev et al., 2006). All rescued viruses were biologically cloned by two or three terminal dilutions and amplified in Vero cells. Virus titers were determined in Vero cells by a plaque-forming assay (PFA) as described previously (Rumyantsev et al., 2006).

Immunoblot analysis

Vero cells in 6-well plates were infected with recombinant viruses at an MOI of 0.5. At 72 h post-infection (p.i.), cell culture supernatants were collected and clarified by centrifugation at $16{,}000 \times g$ for 10 min at 4 °C to remove cell debris. Cells were washed twice with phosphate buffer saline (PBS) and lysed in buffer (25 mM Tris–HCl, pH 7.4, 150 mM NaCl, 1 mM EDTA, 1% NP-40, and 5% glycerol) supplemented with Halt™ Protease Inhibitor Cocktail (Thermo Scientific). Lysates were collected and clarified by centrifugation at $16{,}000 \times g$ for 5 min at 4 °C. Cell culture supernatants or cell lysates were mixed with the 4× protein sample buffer (NuPAGE) supplemented with 10% β-mercaptoethanol, and incubated for 5 min at 95 °C. Proteins were separated by electrophoresis on 4–12% Bis-TrisNuPAGE gel (Invitrogen) with morpholinee than sulfonic acid buffer (Invitrogen) and electro-transferred onto polyvinylidene difluoride membranes (Bio-Rad). After blocking of the membranes with 3% blocking reagent (GE Healthcare Life Sciences) in Tris-buffered saline–0.5% Tween 20 (TBS-T), they were incubated overnight at 4 °C with primary antibodies: (TBEV- or DEN4-specific hyperimmune mouse ascitic fluid (HMAF) at a 1:1000 dilution, ATCC; mouse monoclonal anti-DYKDDDDK Tag (anti-FLAG) antibody at a1:2000 dilution, GenScript Inc.). Membranes were washed in TBS-T and then incubated for 1 h at room temperature in the presence of secondary horseradish peroxidase-conjugated antibodies (GE Healthcare Life Sciences). Membranes were developed with the ECL™-Prime Western detection reagent (GE Healthcare Life Sciences) and bands were visualized on Kodak BiomaxMR film.

Kinetics of virus growth in primary neuronal cells

Primary rat neurons (Gibco) were grown in BD BioCoat 8-well glass slides (BD Biosciences) (10^5 cells/chamber) for 8 days according to the manufacturer's protocol and then infected with viruses at an MOI of 0.1. Cell supernatants were collected at days 3 and 4 p.i. and virus titers were determined in Vero cells. Viral RNA was extracted from cell supernatants and used for sequence analysis. Virus-infected cells on glass slides were fixed with 4% paraformaldehyde and processed for detection of viral antigens as described previously (Heiss et al., 2011).

Evaluation of viruses in mice

Studies in mice were performed at the Animal BSL-3 facilities, in compliance with the guidelines of the NIAID Institutional Animal Care and Use Committee, as described previously (Heiss et al., 2012). Briefly, for virus neurovirulence evaluation, litters of 9 or 10 3-day-old Swiss Webster mice (Taconic Farms) were inoculated intracerebrally (IC) with 10, 10^2, or 10^3 PFU of corresponding virus and monitored for morbidity and mortality up to 21 days p.i. The LD_{50} was determined by the Reed and Muench method (Reed and Muench, 1938). Moribund (paralyzed) mice were euthanized and their brain homogenates were prepared as described previously (Engel et al., 2010; Pletnev et al., 2006). Viral

RNA was extracted from brain homogenates, and the sequence of the genomic region containing engineered miRNA-targets was determined. On day 22 p.i. surviving mice were euthanized and their brains were collected. Virus presence in brain homogenates was evaluated by direct titration and after one blind passage in Vero cells.

To analyze virus replication and distribution of viral antigens in the brain, as well as to evaluate the extent of virus-induced neuronal damage, 3-day-old mice were inoculated IC with 10^3 PFU of the vE1/A3, vE1/A5, vE2/A3, vE2/A5, or vE3/A5 virus. Control mice were mock-inoculated with Leibovitz's L-15 medium (Invitrogen). For analysis of virus replication, the brains of three mice from each group were collected on days 8, 13, and 20 p.i. Virus titers in brain suspensions were quantitated by titration in Vero cells. Virus RNA was extracted from brain homogenates and used for RT-PCR and sequence analyses. For the analysis of viral antigens and neuronal damage, the brains of three mice from each group were collected on days 13 and 20 p.i. In addition, the brains of three mice inoculated IC with 10^3 PFU of the parental TBEV/DEN4 were collected when the mice became moribund (day 6 p.i.) to serve as a positive control. All brains were histologically processed using MultiBrain Technology (NeuroScience Associates) and analyzed by immunohistochemistry for presence of TBEV antigens, microglial activation, and integrity of neuronal somato-dendritic compartments as previously described (Heiss et al., 2012).

Immunogenicity and protective efficacy of miRNA-target viruses were assessed in 3-week-old Swiss Webster female mice. Mice were inoculated intraperitoneally (IP) with 10^5 PFU of each virus, and sera were collected on day 28 p.i. to evaluate neutralizing antibody response. TBEV-specific neutralizing antibody titers were determined by the 60% plaque reduction neutralization assay ($PRNT_{60\%}$) in Vero cells as previously described (Pletnev et al., 2001; Rumyantsev et al., 2006). The neutralizing antibody titer was defined as the dilution of serum that neutralized 60% of the TBEV/DEN4 virus used in the assay. Mice were challenged IP on day 29 with 100 IP LD_{50} (3200 PFU) of the neuroinvasive TBEV/LGT virus, and observed for morbidity and mortality for an additional 4 weeks.

Acknowledgments

We thank Dr. E. Ehrenfeld for critical reading of the paper.

This work was supported by the Division of Intramural Research Program of the National Institute of Allergy and Infectious Diseases, National Institutes of Health.

We do not have any conflict of financial or other interest.

Appendix A. Supporting information

Supplementary data associated with this article can be found in the online version at http://dx.doi.org/10.1016/j.virol.2014.04.001.

References

Barnes, D., Kunitomi, M., Vignuzzi, M., Saksela, K., Andino, R., 2008. Harnessing endogenous miRNAs to control virus tissue tropism as a strategy for developing attenuated virus vaccines. Cell Host Microbe 4, 239–248.

Bartel, D.P., 2009. MicroRNAs: target recognition and regulatory functions. Cell 136, 215–233.

Bonaldo, M.C., Mello, S.M., Trindade, G.F., Rangel, A.A., Duarte, A.S., Oliveira, P.J., Freire, M.S., Kubelka, C.F., Galler, R., 2007. Construction and characterization of recombinant flaviviruses bearing insertions between E and NS1 genes. Virol. J. 4, 115.

Cawood, R., Chen, H.H., Carroll, F., Bazan-Peregrino, M., van Rooijen, N., Seymour, L.W., 2009. Use of tissue-specific microRNA to control pathology of wild-type adenovirus without attenuation of its ability to kill cancer cells. PLoS Pathog. 5, e1000440.

Cawood, R., Wong, S.L., Di, Y., Baban, D.F., Seymour, L.W., 2011. MicroRNA controlled adenovirus mediates anti-cancer efficacy without affecting endogenous microRNA activity. PLoS One 6, e16152.

Edge, R.E., Falls, T.J., Brown, C.W., Lichty, B.D., Atkins, H., Bell, J.C., 2008. A let-7 microRNA-sensitive vesicular stomatitis virus demonstrates tumor-specific replication. Mol. Ther. 16, 1437–1443.

Engel, A.R., Rum yantsev, A.A., Maximova, O.A., Speicher, J.M., Heiss, B., Murphy, B.R., Pletnev, A.G., 2010. The neurovirulence and neuroinvasiveness of chimeric tick-borne encephalitis/dengue virus can be attenuated by introducing defined mutations into the envelope and NS5 protein genes and the 3′ non-coding region of the genome. Virology 405, 243–252.

Fang, Z., Rajewsky, N., 2011. The impact of miRNA target sites in coding sequences and in 3′UTRs. PLoS One 6, e18067.

Filipowicz, W., Bhattacharyya, S.N., Sonenberg, N., 2008. Mechanisms of post-transcriptional regulation by microRNAs: are the answers in sight? Nat. Rev. Genet. 9, 102–114.

Fritz, R., Blazevic, J., Taucher, C., Pangerl, K., Heinz, F.X., Stiasny, K., 2011. The unique transmembrane hairpin of flavivirus fusion protein E is essential for membrane fusion. J. Virol. 85, 4377–4385.

Griffin, D.E., 2003. Immune responses to RNA-virus infections of the CNS. Nat. Rev. Immunol. 3, 493–502.

Heiss, B.L., Maximova, O.A., Pletnev, A.G., 2011. Insertion of microRNA targets into the flavivirus genome alters its highly neurovirulent phenotype. J. Virol. 85, 1464–1472.

Heiss, B.L., Maximova, O.A., Thach, D.C., Speicher, J.M., Pletnev, A.G., 2012. MicroRNA targeting of neurotropic flavivirus: effective control of virus escape and reversion to neurovirulent phenotype. J. Virol. 86, 5647–5659.

Kelly, E.J., Hadac, E.M., Cullen, B.R., Russell, S.J., 2010a. MicroRNA antagonism of the picornaviral life cycle: alternative mechanisms of interference. PLoS Pathog. 6, e1000820.

Kelly, E.J., Hadac, E.M., Greiner, S., Russell, S.J., 2008. Engineering microRNA responsiveness to decrease virus pathogenicity. Nat. Med. 14, 1278–1283.

Kelly, E.J., Nace, R., Barber, G.N., Russell, S.J., 2010b. Attenuation of vesicular stomatitis virus encephalitis through microRNA targeting. J. Virol. 84, 1550–1562.

Kelly, E.J., Russell, S.J., 2009. MicroRNAs and the regulation of vector tropism. Mol. Ther. 17, 409–416.

Krichevsky, A.M., King, K.S., Donahue, C.P., Khrapko, K., Kosik, K.S., 2003. A microRNA array reveals extensive regulation of microRNAs during brain development. RNA 9, 1274–1281.

Lagos-Quintana, M., Rauhut, R., Yalcin, A., Meyer, J., Lendeckel, W., Tuschl, T., 2002. Identification of tissue-specific microRNAs from mouse. Curr. Biol. 12, 735–739.

Langlois, R.A., Albrecht, R.A., Kimble, B., Sutton, T., Shapiro, J.S., Finch, C., Angel, M., Chua, M.A., Gonzalez-Reiche, A.S., Xu, K., Perez, D., Garcia-Sastre, A., Tenoever, B.R., 2013. MicroRNA-based strategy to mitigate the risk of gain-of-function influenza studies. Nat. Biotechnol. 9, 844–847.

Langlois, R.A., Varble, A., Chua, M.A., Garcia-Sastre, A., tenOever, B.R., 2012. Hematopoietic-specific targeting of influenza A virus reveals replication requirements for induction of antiviral immune responses. Proc. Natl. Acad. Sci. U.S.A. 109, 12117–12122.

Lauring, A.S., Jones, J.O., Andino, R., 2010. Rationalizing the development of live attenuated virus vaccines. Nat. Biotechnol. 28, 573–579.

Leber, M.F., Bossow, S., Leonard, V.H., Zaoui, K., Grossardt, C., Frenzke, M., Miest, T., Sawall, S., Cattaneo, R., von Kalle, C., Ungerechts, G., 2011. MicroRNA-sensitive oncolytic measles viruses for cancer-specific vector tropism. Mol. Ther. 19, 1097–1106.

Lin, H.R., Ganem, D., 2011. Viral microRNA target allows insight into the role of translation in governing microRNA target accessibility. Proc. Natl. Acad. Sci. U.S.A. 108, 5148–5153.

Lindenbach, B., Thiel, H., Rice, C.M., 2007. Flaviviridae: the viruses and their replication. In: Knipe, D.M., Howley, P.M. (Eds.), Fields Virology, 5th ed. Lippincott, Williams & Wilkins, Philadelphia, PA, pp. 1101–1152.

Mandl, C.W., 2005. Steps of the tick-borne encephalitis virus replication cycle that affect neuropathogenesis. Virus Res. 111, 161–174.

Mrass, P., Weninger, W., 2006. Immune cell migration as a means to control immune privilege: lessons from the CNS and tumors. Immunol. Rev. 213, 195–212.

Ousman, S.S., Kubes, P., 2012. Immune surveillance in the central nervous system. Nat. Neurosci. 15, 1096–1101.

Pangerl, K., Heinz, F.X., Stiasny, K., 2011. Mutational analysis of the zippering reaction during flavivirus membrane fusion. J. Virol. 85, 8495–8501.

Pasquinelli, A.E., 2012. MicroRNAs and their targets: recognition, regulation and an emerging reciprocal relationship. Nat. Rev. Genet. 13, 271–282.

Perez, J.T., Pham, A.M., Lorini, M.H., Chua, M.A., Steel, J., tenOever, B.R., 2009. MicroRNA-mediated species-specific attenuation of influenza A virus. Nat. Biotechnol. 27, 572–576.

Pham, A.M., Langlois, R.A., TenOever, B.R., 2012. Replication in cells of hematopoietic origin is necessary for Dengue virus dissemination. PLoS Pathog. 8, e1002465.

Pletnev, A.G., 2001. Infectious cDNA clone of attenuated Langat tick-borne flavivirus (strain E5) and a 3′ deletion mutant constructed from it exhibit decreased neuroinvasiveness in immunodeficient mice. Virology 282, 288–300.

Pletnev, A.G., Bray, M., Hanley, K.A., Speicher, J., Elkins, R., 2001. Tick-borne Langat/mosquito-borne dengue flavivirus chimera, a candidate live attenuated vaccine for protection against disease caused by members of the tick-borne encephalitis virus complex: evaluation in rhesus monkeys and in mosquitoes. J. Virol. 75, 8259–8267.

Pletnev, A.G., Bray, M., Huggins, J., Lai, C.J., 1992. Construction and characterization of chimeric tick-borne encephalitis/dengue type 4 viruses. Proc. Natl. Acad. Sci. U.S.A. 89, 10532–10536.

Pletnev, A.G., Swayne, D.E., Speicher, J., Rumyantsev, A.A., Murphy, B.R., 2006. Chimeric West Nile/dengue virus vaccine candidate: preclinical evaluation in mice, geese and monkeys for safety and immunogenicity. Vaccine 24, 6392–6404.

Reed, L.J., Muench, H., 1938. A simple method of estimating fifty per cent endpoint. Am. J. Epidemiol. 27, 493–497.

Rumyantsev, A.A., Chanock, R.M., Murphy, B.R., Pletnev, A.G., 2006. Comparison of live and inactivated tick-borne encephalitis virus vaccines for safety, immunogenicity and efficacy in rhesus monkeys. Vaccine 24, 133–143.

Saetrom, P., Heale, B.S., Snove Jr., O., Aagaard, L., Alluin, J., Rossi, J.J., 2007. Distance constraints between microRNA target sites dictate efficacy and cooperativity. Nucleic Acids Res. 35, 2333–2342.

Sips, G.J., Wilschut, J., Smit, J.M., 2012. Neuroinvasive flavivirus infections. Rev. Med. Virol. 22, 69–87.

Stiasny, K., Kiermayr, S., Bernhart, A., Heinz, F.X., 2013. The membrane-proximal "stem" region increases the stability of the flavivirus e protein postfusion trimer and modulates its structure. J. Virol. 87, 9933–9938.

tenOever, B.R., 2013. RNA viruses and the host microRNA machinery. Nat. Rev. Microbiol. 11, 169–180.

Trindade, G.F., de Santana, M.G., dos Santos, J.R., Galler, R., Bonaldo, M.C., 2012. Retention of a recombinant GFP protein expressed by the yellow fever 17D virus in the E/NS1 intergenic region in the endoplasmic reticulum. Mem. Inst. Oswaldo Cruz 107, 262–272.

Yen, L.C., Lin, Y.L., Sung, H.H., Liao, J.T., Tsao, C.H., Su, C.M., Lin, C.K., Liao, C.L., 2013. Neurovirulent flavivirus can be attenuated in mice by incorporation of neuron-specific microRNA recognition elements into viral genome. Vaccine 31, 5915–5922.

Ylosmaki, E., Hakkarainen, T., Hemminki, A., Visakorpi, T., Andino, R., Saksela, K., 2008. Generation of a conditionally replicating adenovirus based on targeted destruction of E1A mRNA by a cell type-specific microRNA. J. Virol. 82, 11009–11015.

Ylosmaki, E., Martikainen, M., Hinkkanen, A., Saksela, K., 2013. Attenuation of Semliki Forest virus neurovirulence by microRNA-mediated detargeting. J. Virol. 87, 335–344.